Scaling solutions in Bianchi I models with anisotropic stress

Lucas C. Monteiro*
*Departamento de Física and Instituto de Astrofísica e Ciências do Espaço, Universidade de Lisboa, Faculdade de Ciências, Edifício C8, Campo Grande, 1769-016 Lisboa, Portugal**

Abstract
In the present work, we review some features of the Bianchi I metric and study the possibility of different scaling solutions when simpler axisymmetric models are considered. We consider the presence of a single fluid with anisotropic stresses. Expansion normalized variables and change of time variable are advisable and used in the work. In order to study the dynamics, the obtained models are compared with the current supernovae type Ia data and ΛCDM cosmological model to constain the model parameters. Optimal data constraints remain to be imposed for the different case studies. A present time shear abundance is predicted in the order of 0.001. To the best of our knowledge our results are novel.

1. INTRODUCTION

Named after Luigi Bianchi, who classified the relevant 3-dimensional spaces, Bianchi universes are the class of cosmological models that are homogeneous but not necessarily isotropic, that is the rate of its expansion can be different when measured along different axes.

The simplest examples of Bianchi universes are known as 'Type I', which are a generalisation of the Minkowski flat metric to the case with separate scale factors in each cartesian direction:

$$\mathrm{d}s^2 = -c^2\mathrm{d}t^2 + A^2(t)\mathrm{d}x^2 + B^2(t)\mathrm{d}y^2 + C^2(t)\mathrm{d}z^2 \quad (1)$$

where we will adopt the convention that the speed of light $\boldsymbol{c = 1}$ and $\boldsymbol{A(t)}$, $\boldsymbol{B(t)}$ and $\boldsymbol{C(t)}$ are well behaved functions of the cosmic time $\boldsymbol{t}$, and only depend on the latter.

From this metric we obtain the following Einstein field equations:

$$\begin{aligned}
\frac{\dot{A}\dot{B}}{AB} + \frac{\dot{B}\dot{C}}{BC} + \frac{\dot{C}\dot{A}}{CA} &= \kappa^2\rho \\
\frac{\dot{B}\dot{C}}{BC} + \frac{\ddot{B}}{B} + \frac{\ddot{C}}{C} &= -\kappa^2(\mathrm{p_{iso.}} + \Pi_1) \\
\frac{\dot{C}\dot{A}}{CA} + \frac{\ddot{C}}{C} + \frac{\ddot{A}}{A} &= -\kappa^2(\mathrm{p_{iso.}} + \Pi_2) \\
\frac{\dot{A}\dot{B}}{AB} + \frac{\ddot{A}}{A} + \frac{\ddot{B}}{B} &= -\kappa^2(\mathrm{p_{iso.}} + \Pi_3)
\end{aligned} \quad (2)$$

Again we will adopt the convention that the Einstein gravitational constant $\boldsymbol{\kappa = 1}$ and consider the matter fields to be a fluid with a energy-density $\boldsymbol{\rho(t)}$, an isotropic pressure $\mathbf{p_{iso.}} \equiv \boldsymbol{p(t)}$, and also anisotropic stresses which are described by a diagonal matrix $\boldsymbol{\Pi_{ab}}$:

$$\Pi^b_a = \begin{pmatrix} 0 & 0 & 0 & 0 \\ 0 & -\Pi_1 & 0 & 0 \\ 0 & 0 & -\Pi_2 & 0 \\ 0 & 0 & 0 & -\Pi_3 \end{pmatrix} . \quad (3)$$

with null trace, i.e., $\Pi_1 + \Pi_2 + \Pi_3 = 0$.

Applying conservation equations to the fluid we derive [1]:

$$\dot{\rho} + (\rho + p)\left(\frac{\dot{A}}{A} + \frac{\dot{B}}{B} + \frac{\dot{C}}{C}\right) + \sigma_{ab}\Pi^{ab} = 0 \quad (4)$$

where $\boldsymbol{\sigma_{ab}}$ is the shear tensor which accounts for the time evolution of distortion, and it is another traceless matrix:

$$\sigma^b_a = \begin{pmatrix} 0 & 0 & 0 & 0 \\ 0 & \sigma_1 & 0 & 0 \\ 0 & 0 & \sigma_2 & 0 \\ 0 & 0 & 0 & \sigma_3 \end{pmatrix} \quad (5)$$

Also, defining $S^3 = A(t)B(t)C(t)$ so that $S(t)$ is the average scale factor of the Bianchi I universe, we have that:

$$\frac{\dot{A}}{A} + \frac{\dot{B}}{B} + \frac{\dot{C}}{C} = \frac{(ABC)^{\cdot}}{ABC} = 3\,\frac{\dot{S}}{S} = \theta \quad (6)$$

where $\boldsymbol{\theta(t)}$ is called the expansion and is proportional to the average Hubble factor, $\boldsymbol{H}$:

$$H = \frac{\dot{S}}{S} \;\Rightarrow\; \theta = 3H. \quad (7)$$

An advisable change of time variable is to consider the so-called number of e-folding, defined by:

$$\frac{\mathrm{d}}{\mathrm{d}t} = \frac{\mathrm{d}\tau}{\mathrm{d}t}\frac{\mathrm{d}}{\mathrm{d}\tau} = H\frac{\mathrm{d}}{\mathrm{d}\tau} = \frac{\theta}{3}\frac{\mathrm{d}}{\mathrm{d}\tau}\,, \quad \tau = \ln\frac{S}{S_0} \quad (8)$$

2. COSMOLOGICAL CONSTANT

A non-coupled cosmological constant $\boldsymbol{\rho_\Lambda}$ will be considered, making:

$$\rho = \rho_m + \rho_\Lambda \quad (9)$$

where $\boldsymbol{\rho_m}$ is the matter-density parameter.

* fc52849@alunos.fc.ul.pt

From Eqs. (4) and (6), we obtain the equations of evolution of ρ_m and ρ_Λ:

$$\dot{\rho}_m + (\rho_m + p_m)\,\theta + \sigma_{ab}\Pi^{ab} = 0 \tag{10}$$
$$\dot{\rho}_\Lambda + (\rho_\Lambda + p_\Lambda)\,\theta = 0 \tag{11}$$

where there is no coupling in the time evolution of ρ_Λ.

It is widely assumed that it is justified to take the *equation of state*, $p = w\,\rho$, for each species - p_m and p_Λ - where $\boldsymbol{w}$ is the equation of state parameter and constant, which belongs to the interval $-1 \leq w \leq 1$. This corresponds to consider that the matter/radiation content is a fluid with anisotropic stresses.

The time evolution of ρ_m can be simplified:

$$\dot{\rho}_m + \rho_m\,(1 + w_m)\,\theta + \sigma_{ab}\Pi^{ab} = 0 \tag{12}$$

where w_m will take the values for dust or radiation. As we consider a single fluid, we define $\boldsymbol{w_m} \equiv w$, in order to simplify the writing.

This parameter takes some special values:

- $w = 0$ means $p = 0$ or that the pressure is negligible with respect to the density, for example, non-relativistic matter, or simply *dust*;
- $w = 1/3$ is relativistic matter, or *radiation*;
- $w = -1$ corresponds to the cosmological constant.

This way we verify that ρ_Λ is indeed a constant:

$$\dot{\rho}_\Lambda + (\rho_\Lambda + p_\Lambda)\,\theta = \rho'_\Lambda + 3\,\rho_\Lambda(1 + w_\Lambda) = 0 \;\Rightarrow\; \rho'_\Lambda = 0 \tag{13}$$

using the advised time variable change of Eq. (8).

3. AXISYMMETRIC BIANCHI I MODELS

Consider now the interesting case of axisymmetric Bianchi I models in which $B(t) = C(t)$ and thus we only have 2 scale factors, $A(t)$ and $B(t)$ instead of 3 scale factors. Knowing that $\sigma_1 + \sigma_2 + \sigma_3 = 0$ and $\Pi_1 + \Pi_2 + \Pi_3 = 0$, we can simplify our shear and anisotropic stresses matrixes with:

$$\begin{aligned} \sigma_2 = \sigma_3 = \sigma_\perp \;&\Rightarrow\; \sigma_1 = \sigma_{||} = -2\sigma_\perp \\ \Pi_2 = \Pi_3 = \Pi_\perp \;&\Rightarrow\; \Pi_1 = \Pi_{||} = -2\Pi_\perp \end{aligned} \tag{14}$$

Therefore we derive the trace of $\sigma_{ab}\sigma^{ba} = 6\sigma_\perp^2$.

$$\begin{aligned} \sigma_{ab}\sigma^{bc} &= \begin{pmatrix} 0 & 0 & 0 & 0 \\ 0 & \sigma_1\sigma_1 & 0 & 0 \\ 0 & 0 & \sigma_2\sigma_2 & 0 \\ 0 & 0 & 0 & \sigma_3\sigma_3 \end{pmatrix} \\ &= \begin{pmatrix} 0 & 0 & 0 & 0 \\ 0 & 4\sigma_\perp^2 & 0 & 0 \\ 0 & 0 & \sigma_\perp^2 & 0 \\ 0 & 0 & 0 & \sigma_\perp^2 \end{pmatrix} \end{aligned} \tag{15}$$

And similarly the trace of $\sigma_{ab}\Pi^{ab} = -6\sigma_\perp\Pi_\perp$.

$$\begin{aligned} \sigma_{ab}\Pi^{bc} &= \begin{pmatrix} 0 & 0 & 0 & 0 \\ 0 & \sigma_1\Pi_1 & 0 & 0 \\ 0 & 0 & \sigma_2\Pi_2 & 0 \\ 0 & 0 & 0 & \sigma_3\Pi_3 \end{pmatrix} \\ &= \begin{pmatrix} 0 & 0 & 0 & 0 \\ 0 & -4\sigma_\perp\Pi_\perp & 0 & 0 \\ 0 & 0 & -\sigma_\perp\Pi_\perp & 0 \\ 0 & 0 & 0 & -\sigma_\perp\Pi_\perp \end{pmatrix} \end{aligned} \tag{16}$$

Notice that in the literature one defines $\sigma_{ab}\sigma^{ab} = 2\sigma^2$. So we see that in the axisymmetric case $\sigma^2 = 3\sigma_\perp^2$ and $\sigma_{ab}\Pi^{ab} = -2\sqrt{3}\sigma\Pi_\perp$.

Knowing that, we rewrite Eq. (12) as:

$$\dot{\rho}_m + \rho_m\,(1 + w)\,\theta - 2\sqrt{3}\,\sigma\Pi_\perp = 0 \tag{17}$$

The other two field equations that were used are derived introducing the kinematical quantities - vorticity tensor w_{ab}, the expansion θ, shear tensor σ_{ab} and the acceleration vector $\dot{u}^a$ [1] - in the Einstein equations, yielding:

$$\dot{\sigma} + \theta\,\sigma + \sqrt{3}\,\kappa^2\Pi_\perp = 0 \tag{18}$$
$$\dot{\theta} + \frac{\theta^2}{3} + 2\sigma^2 + \kappa^2\left(\frac{\rho + 3p}{2}\right) = 0 \tag{19}$$

and the resulting Friedmann constraint:

$$\frac{\theta^2}{3} = \kappa^2\rho + \sigma^2 \tag{20}$$

Only equations Eq. (17) and Eq. (18) will be used while equation Eq. (19) will not. Instead, the values of θ will be calculated using Eq. (20) and the calculated values of ρ and σ.

We then arrive at the system that will be studied, where the change of time variable in Eq. (8) was applied:

$$\begin{cases} \rho'_m + 3\,\rho_m\,(1 + w) - 6\sqrt{3}\,\sigma\,\Pi_\perp/\theta = 0 \\ \\ \sigma' + 3\,\sigma + 3\sqrt{3}\,\Pi_\perp/\theta = 0 \\ \\ \theta = \sqrt{3\,(\,\rho_m + \rho_\Lambda + \sigma^2)} \end{cases} \tag{21}$$

Notice that the dimensions of the variables are satisfied. θ and σ have H of dimension while ρ_m, ρ_Λ and $\Pi_\perp$, dimension H^2.

This system considers a single fluid, represented by the w equation of state parameter. It allows possible

interactions between baryonic matter and dark matter, being that a fluid that consists of 'collisionless' particles.

Now that the theoretical background of the work is laid down, the next chapters consist on its analysis and examination, as well as the comparison with other cosmological models.

4. EXPANSION NORMALIZED VARIABLES

Dividing Eq. (20) by $\theta^2/3$ on both sides, we define two new dimensionless variables - $\boldsymbol{x}$ and $\boldsymbol{y}$ - that will be extensively used in the sections where scaling solutions are calculated.

$$1 = \frac{3\rho}{\theta^2} + \frac{3\sigma^2}{\theta^2} \;\Leftrightarrow\; x^2 + y^2 = 1 \tag{22}$$

defining:

$$x^2 \equiv \frac{3\rho}{\theta^2}\,, \qquad y^2 \equiv \frac{3\sigma^2}{\theta^2} \tag{23}$$

Notice that the system is now seen as in a circle. This new variables are particularly convenient to use in our study, considering that if x, or y, are at an equilibrium point, that is when $\dot{x} = 0$, or $\dot{y} = 0$, then the variables σ^2, ρ and θ^2 are all evolving with fixed proportions to each other or, in other words, we have a so-called *scaling solution*.

So the derivatives of x and y were easily calculated using logarithmic differentiation:

$$2\frac{\dot{x}}{x} = \frac{\dot{\rho}}{\rho} - 2\frac{\dot{\theta}}{\theta}\,, \qquad \frac{\dot{y}}{y} = \frac{\dot{\sigma}}{\sigma} - \frac{\dot{\theta}}{\theta} \tag{24}$$

This equations were then manipulated in a way that their depence is only of x, y, w and reduced $\Pi_\perp$, or $\boldsymbol{\Pi_\perp^{red.}}$, that is just a dimensionless parameter defined by:

$$\Pi_\perp = \Pi_\perp^{\text{red.}}\theta^2 \tag{25}$$

Considering Eqs. (17), (18), (19) and (23):

$$x' = \frac{1}{4}(1+3w)\,x\,(x^2-2) + 2y^2x + 9\,\Pi_\perp^{\text{red.}}\,\frac{y}{x} \tag{26}$$

$$y' = 2\,y^3 + \left(\frac{x^2}{2}(1+3w) - 2\right)y - 9\,\Pi_\perp^{\text{red.}} \tag{27}$$

However both equations need not be used due to the relation between x and y - Eq. (22) - so we choose the simplest of them, Eq. (27), and study solely its points of equilibrium. Substituting then x^2 with $1-y^2$, yields our study function:

$$y' = \frac{3}{2}(1-w)\,y\,(y^2-1) - 9\,\Pi_\perp^{\text{red.}} \tag{28}$$

5. SCALING SOLUTIONS OF DUST

In this section we seek scaling regimes for different anisotropic stress cases. These solutions are important since they are remarkable cases where the shear is porpotional to the other energy density parameters, allowing to determine the situations where it grows, or decreases, in relation to them.

As previously discussed, to find the scaling solutions we will need to find the values of y, w and $\Pi_\perp^{\text{red.}}$ where Eq. (28) is equal to zero. Furthermore only the points of equilibrium that are stable are considered. This condition is verified when $y'' \equiv \frac{\partial y'}{\partial y}$ is negative.

Knowing that, we can start studying different cases of $\Pi_\perp$, and calculating which values can the different parameters take to yield stable scaling solutions. We will particulary consider dust solutions, that is $w = 0$.

In all the following cases the evolution of the cosmological parameters - ρ, σ and θ - are calculated using Eq. (21) from the initial time $\boldsymbol{\tau_i}$ until final time $\boldsymbol{\tau_f}$. In this work the values of time are usually defined as:

$$\tau_i = -14\,, \qquad \tau_f = 0 \tag{29}$$

spanning a considerable period of time from a distant past until the present.

To simulate this evolution the cosmological parameters initial values of the cosmological parameters need to be inputed as well. The initial value of ρ_m, or $\boldsymbol{\rho_{mi}}$, is calculated considering its time evolution equation in isotropic models, or Eq. (12) without the coupling parameter. This can be seen as the anisotropic stresses only 'kicking in' the instant after the beginning of the universe. This way:

$$\begin{aligned} \dot{\rho}_m + \rho_m\,(1+w)\,\theta = 0 \;&\Leftrightarrow \\ \rho_m' = \frac{\mathrm{d}\rho_m}{\mathrm{d}\tau} = -3\,\rho_m\,(1+w) \;&\Rightarrow \\ \rho_{mi} = \Omega_{m0}\,\rho_0\,e^{-3\,(1+w)\,\tau_i} \end{aligned} \tag{30}$$

The different energy-density abundance parameters $\boldsymbol{\Omega}$ are defined as:

$$\begin{aligned} \Omega_m &= \frac{3\rho_m}{\theta^2} \\ \Omega_\Lambda &= \frac{3\rho_\Lambda}{\theta^2} \\ \Omega_\sigma &= \frac{3\sigma^2}{\theta^2} \end{aligned} \tag{31}$$

The index zero is a representation of the corresponding abundance at present time, so Ω_{m0} corresponds to current matter abundance. We define $\Omega_{m0}\,\rho_0 = 0.3$ considering current observations [2] (at $\tau_i = 0$), making:

$$\rho_{mi} = 0.3\,e^{-3\,\tau_i} \tag{32}$$

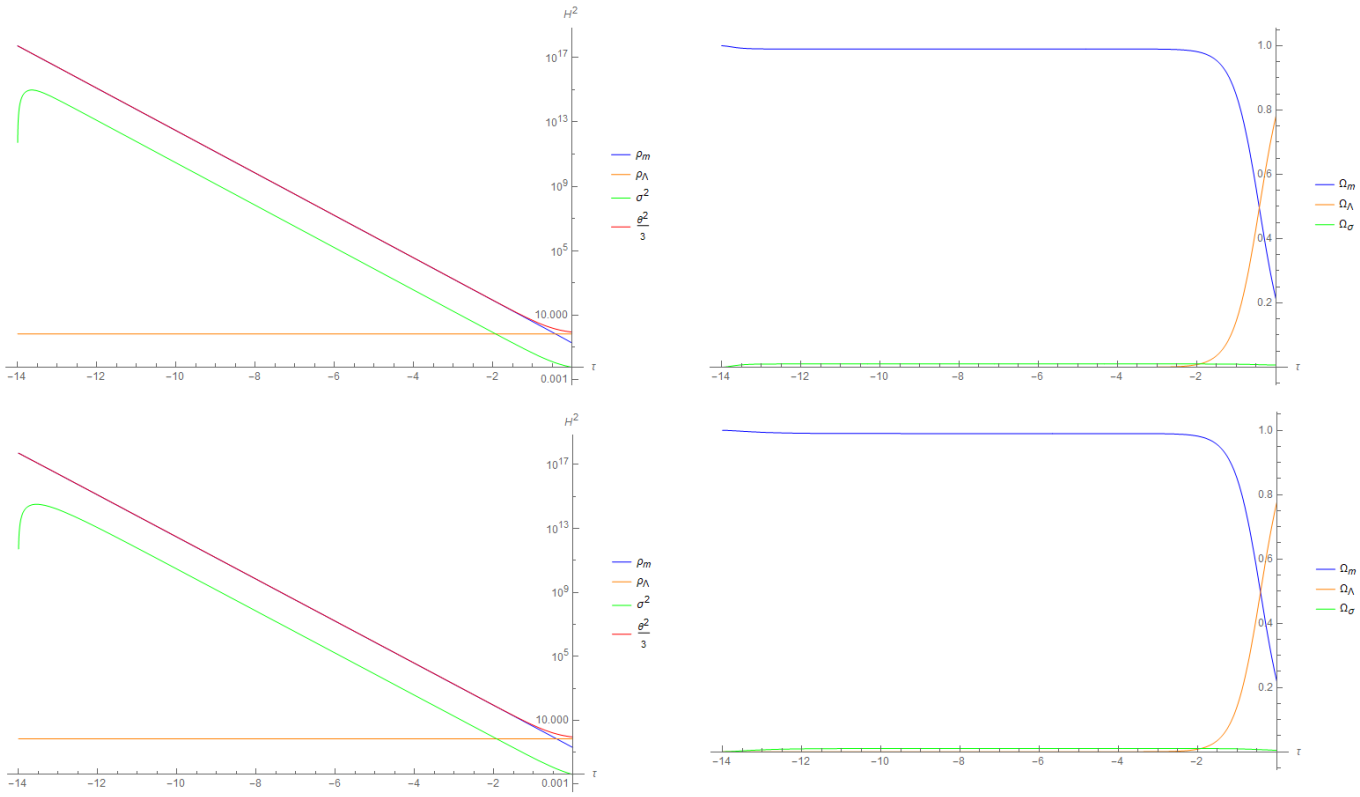

Figure 1. Time evolution of cosmological parameters for dust solutions, i.e., $w = 0$ in different case studies with the system evolving over time from $\tau_i = -14$ to $\tau_f = 0$. **Top** panels: Case study 1 where y_c was defined as $1/10$. **Bottom** panels: Case study 2 where y_c was also defined as $1/10$. However this case needs other parameter to be defined - $\lambda_\perp$ - defined as -1/10. **Left** panels: Evolution of the system's cosmological variables - ρ_m, σ^2 and $\theta^2/3$ - of dimension H^2 as well as $\rho_\Lambda = 0.7$. Both cases yielded aparently similar scaling results, i.e., the cosmological variables evolved proportional to each other. **Right** panels: Evolution of the energy-density abundance parameters - Ω_{m0}, $\Omega_{\sigma 0}$ and $\Omega_{\Lambda 0}$. Analysing the graphs shows us that the abundance is constant while in scaling regime.

since we will consider dust solutions ($w = 0$).

Knowing ρ_{mi} we take the initial value of the shear, or $\boldsymbol{\sigma_i}$, as a smaller value. This value is arbitary and does not influence the calculations because the scaling solution is an *attractor*, or in other words, the system dynamics is not dependent of its starting conditions so the shear values will always stabilize at the same values, proportional to ρ_m.

$$\sigma_i = 10^{-3}\sqrt{\rho_{mi}} \tag{33}$$

where the parameters attain the proper dimension.

The initial expansion parameter, or $\boldsymbol{\theta_i}$, is calculated using the Friedmann constraint of the system, given by Eq. (20):

$$\theta_i = \sqrt{3\,(\,\rho_{mi} + \rho_\Lambda + \sigma_i^2)} \tag{34}$$

This way the initial values of the parameters, that depend only of the initial number of e-folds, τ_i, are approximatly:

$$\begin{aligned} \rho_{mi} &\approx 5.22 \cdot 10^{17}\ , \\ \sigma_i^2 &\approx 5.22 \cdot 10^{11}\ , \\ \theta_i^2/3 &\approx 5.22 \cdot 10^{17} \end{aligned} \tag{35}$$

when $\tau_i = -14$. The initial value of $y \approx 10^{-3}$. The cosmological constant does not change during the evolution of the system, demonstrated in Eq. (13), and is defined as $\rho_\Lambda = 0.7$, by observations.

Four cases will be considered in the next subsections, and the evolution of the resulting systems calculated with the application of expansion normalized variables:

1. $\Pi_\perp = \lambda_\perp \theta^2$
2. $\Pi_\perp = \lambda_\perp\,(\,\rho + \alpha\,\sigma^2\,)$
3. $\Pi_\perp = \lambda_\perp \left(\frac{\rho}{\sigma^2}\right)^\alpha \theta^2$
4. $\Pi_\perp = \lambda_\perp\, \rho^\beta\, (\sigma^2)^\alpha$

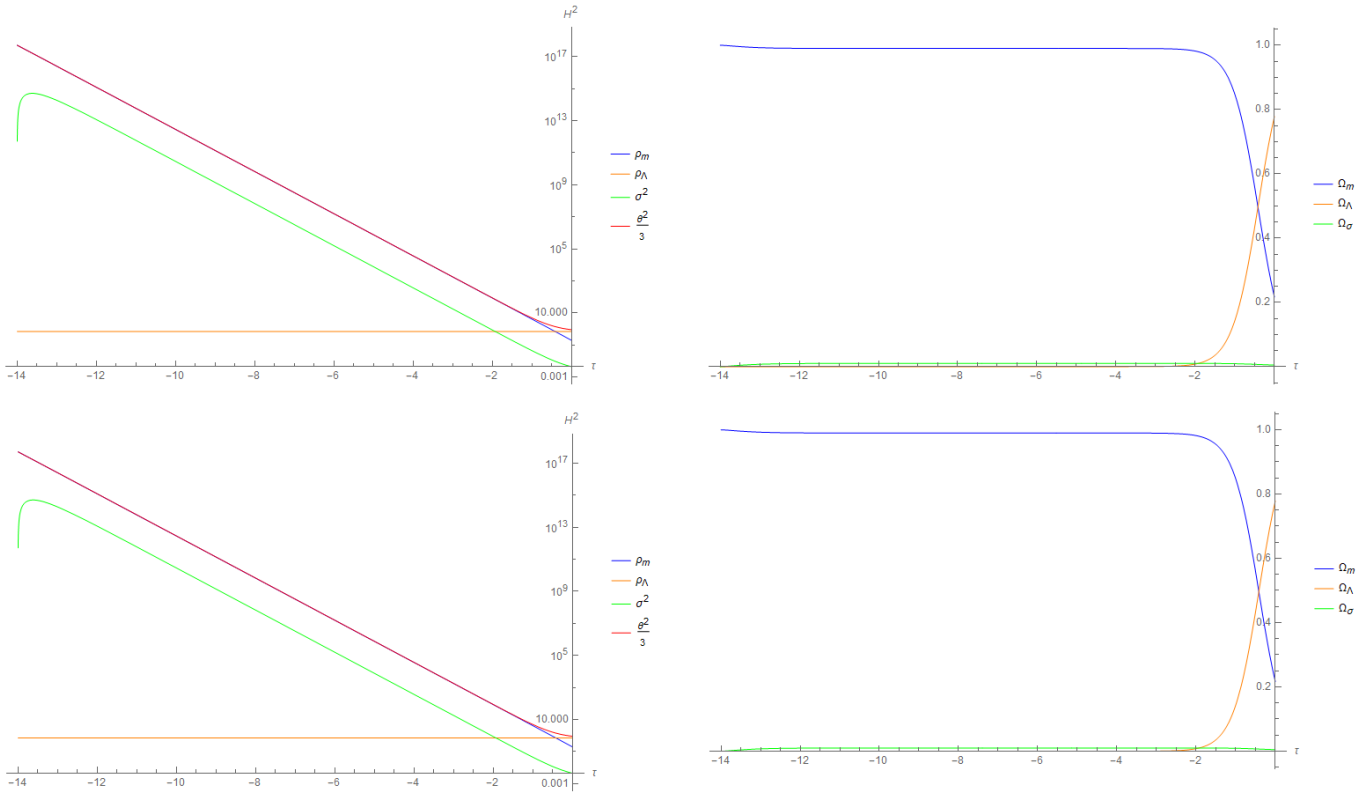

Figure 2. Time evolution of cosmological parameters for dust solutions, i.e., $w = 0$ in different case studies with the system evolving over time from $\tau_i = -14$ to $\tau_f = 0$. **Top** panels: Case study 3 where y_c and α_i were defined as 1/10. **Bottom** panels: Case study 4 where y_c was also defined as 1/10 and α_i as -1/10. **Left** panels: Evolution of the system's cosmological variables - ρ_m, σ^2 and $\theta^2/3$ - of dimension H^2 as well as $\rho_\Lambda = 0.7$. **Right** panels: Evolution of the energy-density abundance parameters - Ω_{m0}, $\Omega_{\sigma 0}$ and $\Omega_{\Lambda 0}$. Both cases yielded very similar scaling solutions results due to the similar nature of this case studies.

To the best of our knowledge, these specific $\Pi_\perp$ forms weren´t previously considered in literature.

5.1 Case 1: $\boldsymbol{\Pi_\perp = \lambda_\perp \theta^2}$

The simplest of all cases is $\Pi_\perp^{\text{red.}} = \lambda_\perp$ [remember Eq. (25)], where $\boldsymbol{\lambda_\perp}$ is a constant, and will be the first case in consideration. Points of equilibrium, or critical points $\boldsymbol{y_c}$, are found when $y' = 0$:

$$\lambda_\perp = \frac{1}{6}(1-w)\, y_c\, (y_c^2 - 1) \tag{36}$$

and studying the stability of those points we get $y'' < 0$:

$$\begin{aligned} w < 1 \ \wedge \ y_c^2 < \frac{1}{3} \\ w > 1 \ \wedge \ y_c^2 > \frac{1}{3} \end{aligned} \tag{37}$$

As w is less than 1 in this particular case, and equal to 0, we can choose values of y_c that satisfy $|y_c| < 1/\sqrt{3}$. For example:

$$y_c = \frac{1}{10} \ \Rightarrow \ \lambda_\perp = -\frac{33}{2000} \tag{38}$$

Notice that in this case the signal of $\lambda_\perp$ does not affect the final result since choosing values of y_c with different signals yields the same results.

Defining the wanted critical value of y we can then calculate the $\lambda_\perp$ and consequently the form of $\Pi_\perp$. The system of Eq. (21) is then possible to numerically resolve and the evolution of the cosmological parameters over time can be represented, as in Figure 1.

5.2 Case 2: $\boldsymbol{\Pi_\perp = \lambda_\perp (\rho + \alpha \sigma^2)}$

Manipulating the definition of x and y variables, as in Eq. (23):

$$\rho = \frac{x^2\, \theta^2}{3}\,, \qquad \sigma^2 = \frac{y^2\, \theta^2}{3} \tag{39}$$

$\Pi_\perp^{\text{red.}}$ for this case is simply found:

$$\Pi_\perp^{\text{red.}} = \frac{1}{3}\lambda_\perp (x^2 + \alpha\, y^2) = \frac{1}{3}\lambda_\perp (1 - y^2 + \alpha\, y^2) \tag{40}$$

Similary to Case 1, the points of equilibrium are cal-

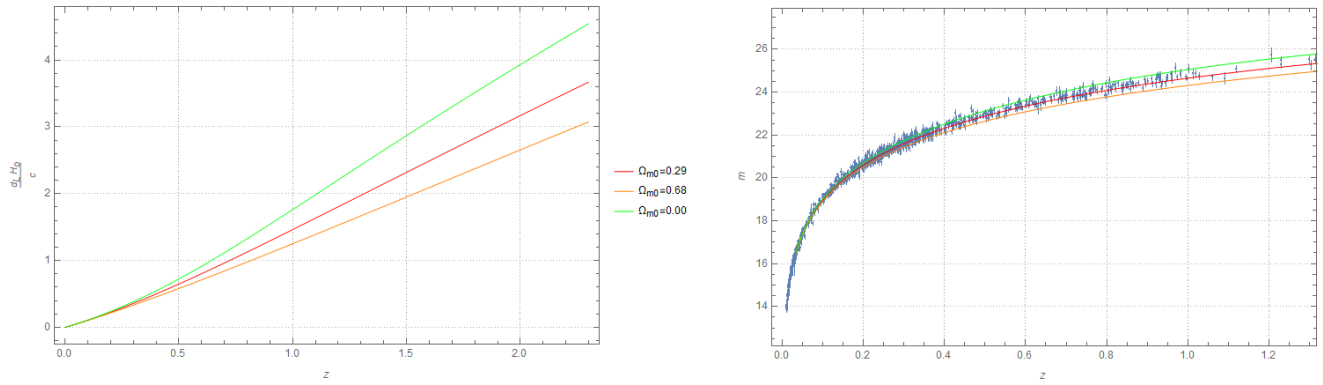

Figure 3. Comparison of different Ω_{m0} values in ΛCDM model. The value of $\Omega_{\sigma 0}$ was fixed and equalled 0.02, and the redshift, z, represented in x-axis varied from 0 to 2. **Left** panel: Luminosity distance versus redshift. **Right** panel: Predicted apparent magnitude versus redshift and observational apparent magnitude data. The observational data points, shown with errorbars, are obtained from SNIa and $H_0 = 68$ km/s/Mpc, $M = -19.4$ and $c = 3 \cdot 10^5$ km/s. The universe with mass density 0.29 provided the best fit with observations.

culated when $y' = 0 \Rightarrow$

$$\alpha = \frac{y_c^2 - 1}{y_c^2} \frac{y_c\,(1-w) + 2\lambda_\perp}{2\lambda_\perp} \tag{41}$$

Notice that in this case the equation was solved for α instead of $\lambda_\perp$. We will always solve for the parameter that yields the simplest results. That being said we verify the stable values, $y'' < 0 \Rightarrow$

$$\begin{aligned} y_c < 0 \wedge \lambda_\perp > -\frac{1}{4}(1-w) y_c (y_c^2+1) \\ y_c > 0 \wedge \lambda_\perp < -\frac{1}{4}(1-w) y_c (y_c^2+1) \end{aligned} \tag{42}$$

with $w \in \mathbb{R}$.

Choosing our critical point example $y_c = 1/10$, Eq. (42) can be resolved, yielding the interval of values that $\lambda_\perp$ can take in way that a scaling solution is obtained:

$$y_c > 0 \;\Rightarrow\; \lambda_\perp < -\frac{101}{4000} \tag{43}$$

therefore we can choose $\lambda_\perp = -1/10$ for example and calculate the intended value of α using Eq. (41).

5.3 Case 3: $\Pi_\perp = \lambda_\perp \left(\frac{\rho}{\sigma^2}\right)^\alpha \theta^2$

Again $\Pi_\perp^{\text{red.}}$ is calculated using Eq. (39):

$$\Pi_\perp^{\text{red.}} = \lambda_\perp \Big(\frac{x^2}{y^2}\Big)^\alpha = \lambda_\perp \Big(\frac{1-y^2}{y^2}\Big)^\alpha \tag{44}$$

Then equation Eq. (28) is equaled to zero to find the scaling solutions points, y_c where $y' = 0$:

$$\lambda_\perp = \frac{1}{6}\,(1-w)\,y_c\,(y_c^2-1)\Big(\frac{1-y_c^2}{y_c^2}\Big)^{-\alpha} \tag{45}$$

and verified if the points are stable ($y'' < 0$):

$$\begin{aligned} w < 1 \;\wedge\; \alpha > \frac{1}{2}(3y_c^2 - 1) \\ w > 1 \;\wedge\; \alpha < \frac{1}{2}(3y_c^2 - 1) \end{aligned} \tag{46}$$

with $y_c \in \mathbb{R}$.

Because we seek dust solutions $\alpha > (3y_c^2 - 1)/2$, so if, for example:

$$y_c = \frac{1}{10} \;\Rightarrow\; \alpha > -\frac{97}{200} \tag{47}$$

Choosing a value of $\alpha = 1/10$ we then calculate the value of $\lambda_\perp$ that corresponds to stable values.

5.4 Case 4: $\Pi_\perp = \lambda_\perp\, \rho^\beta\, (\sigma^2)^\alpha$

In this last case, a β exponent is introduced. However, as previously noted, $\Pi_\perp$ has dimension H^2, so β and α are dependent such that:

$$\alpha + \beta = 1 \;\Rightarrow\; \Pi_\perp = \lambda_\perp\, \rho^{1-\alpha}\, \sigma^{2\alpha} \tag{48}$$

so:

$$\Pi_\perp^{\text{red.}} = \lambda_\perp \Big(\frac{x^2}{3}\Big)^{1-\alpha} \Big(\frac{y^2}{3}\Big)^{\alpha} = \frac{\lambda_\perp}{3}\,(1-y^2)^{1-\alpha}\, y^{2\alpha} \tag{49}$$

The stable points of equilibrium of this case were calculated in the same way as in the others:

$$\lambda_\perp = -\frac{1}{2}\,(1-w)\,y_c \Big(\frac{1-y_c^2}{y_c^2}\Big)^{\alpha} \tag{50}$$

and,

$$\begin{aligned} w < 1 \;\wedge\; \alpha < \frac{1}{2}(1-y_c^2) \\ w > 1 \;\wedge\; \alpha > \frac{1}{2}(1-y_c^2) \end{aligned} \tag{51}$$

where $y_c \in \mathbb{R}$.

Notice that the solutions of this case are very similar to Case 3 because of their similar nature. As in Case 3 $w = 0$ so, choosing our example $y_c = 1/10$ we have:

$$y_c = \frac{1}{10} \;\Rightarrow\; \alpha < \frac{99}{200} \tag{52}$$

However these are purely arbitary values and served only as a proof of concept of the different model cases. Now, constraints on these parameters need to be applied in order to match the current observational data.

6. ΛCDM COSMOLOGICAL MODEL

The ΛCDM, or *Lambda cold dark matter*, model is the simplest model of universe that describes the present acceleration of the universe and fits with the present day cosmological data. As in our model, it is based on the Einstein's theory of general relativity with a spatially flat, homogeneous space-time, however lacks the anisotropic stresses described by Π_{ab} therefore $A(t) = B(t) = C(t)$, i.e., it is isotorpic.

6.1 Energy-density abundance

In this model, the observed acceleration of the universe has been explained by introducing a positive cosmological constant which is mathematically equivalent to a vacuum energy with equation of state parameter $w = -1$, as discussed in Section 2. The Hubble parameter is given as a funtion of redshift, $\boldsymbol{z}$, and in terms of abundances Ω - $\boldsymbol{\Omega_{m0}}$, $\boldsymbol{\Omega_{\sigma 0}}$ and $\boldsymbol{\Omega_{\Lambda 0}}$:

$$H^2 = H_0^2\Big(\,\Omega_{m0}\,(1+z)^3 + \Omega_{\sigma 0}\,(1+z)^6 + \Omega_{\Lambda 0}\,\Big) \tag{53}$$

where due to the flatness of space-time:

$$\Omega_{m0} + \Omega_{\sigma 0} + \Omega_{\Lambda 0} = 1 \tag{54}$$

The ΛCDM model says that the current corresponding values are:

$$\begin{aligned} \Omega_{m0} &\sim 0.3 \\ \Omega_{\Lambda 0} &\sim 0.7 \end{aligned} \tag{55}$$

with the shear parameter $\Omega_{\sigma 0}$ being in the order of 0.01 [3].

6.2 Luminosity distance

In order to analyse the data, the most typical and commonly used current observations are the *type Ia supernovae* (SNIa), and direct measurement of the luminosity distance $\boldsymbol{d_L(z)}$, defined as [3]:

$$\frac{H_0\, d_L(z)}{c} = (1+z)\int_0^z \frac{H_0}{H(z')}\,\mathrm{d}z' \tag{56}$$

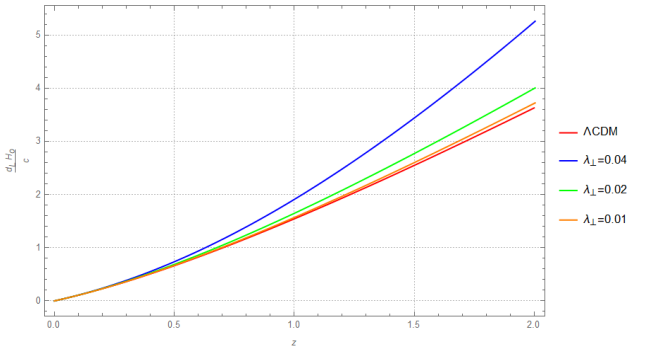

Figure 4. Comparison between ΛCDM and Case 1 Bianchi I cosmological models luminosity distance versus redshift. In ΛCDM model $\Omega_{m0} = 0.3$ and $\Omega_{\Lambda 0} = 0.7$, while in Case 1, $\lambda_\perp$ took different values - 0.04, 0.02 and 0.01. The smaller the value of $\lambda_\perp$, closer the approximation between the models, since the coupling becomes negligible.

where H_0 is the *Hubble's constant*.

Substituting with Eq. (53) we attain the ΛCDM model luminosity distance equation:

$$d_L = \frac{c}{H_0}(1+z)\int_0^z \frac{\mathrm{d}z'}{\sqrt{\Omega_{m0}(1+z')^3 + \Omega_{\sigma 0}(1+z')^6 + \Omega_\Lambda}} \tag{57}$$

that can be solved algebraically.

6.3 Apparent magnitude

The apparent magnitude $\boldsymbol{m(z)}$ of the source, with an absolute magnitude $\boldsymbol{M}$, is related to the luminosity distance, in Megaparsecs, by the formula [3]:

$$m(z) + M = 5\,log_{10}\Big(\frac{d_L(z)}{\mathrm{Mpc}}\Big) + 25 \tag{58}$$

The predicted $m(z)$ can then be compared with the observed $m(z)$ of the SNIa dataset to test the consistency of the theoretical model with observations.

In Figure 3 this is evidenced, where Ω_{m0} took different values. $\Omega_{\sigma 0}$ was defined as 0.02 [3] and Ω_Λ calculated for the different cases using Eq. (54).

When calculating apparent magnitudes, the values of the parameters necessary to compare with observational data are defined as:

$$\begin{aligned} H_0 &= 68\,\mathrm{km/s/Mpc} \\ c &= 3\cdot 10^5\,\mathrm{km/s} \\ M &= -19.4 \end{aligned} \tag{59}$$

7. OBSERVATIONAL CONSTRAINTS

Knowing that the ΛCDM model offers a good fit in current observational data and how to predict appar-

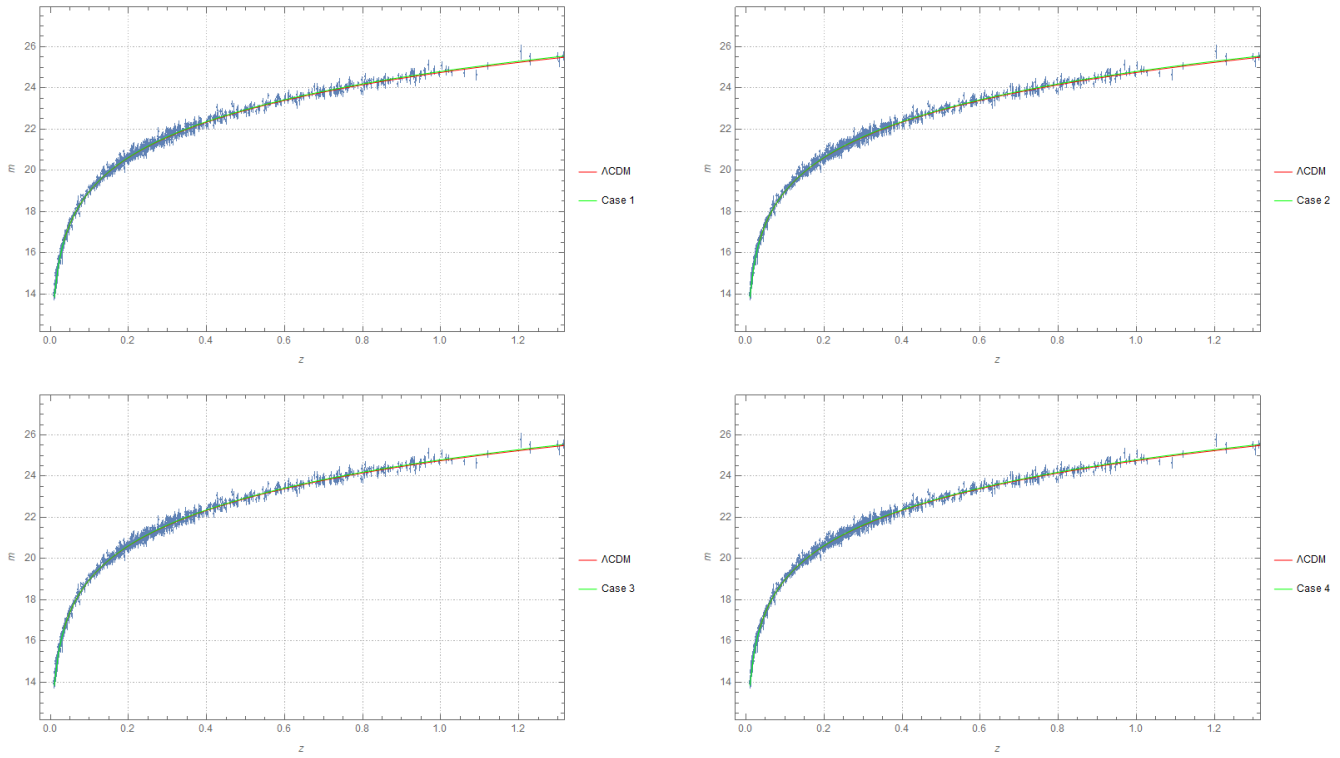

Figure 5. Comparison of predicted apparent magnitude m of different Bianchi I scaling models with $\alpha = 0.1$ and ΛCDM and observational apparent magnitude data versus redshift z. The observational data points, shown with errorbars, are obtained from SNIa and $H_0 = 68$ km/s/Mpc, $M = -19.4$ and $c = 3 \cdot 10^5$ km/s. **Top left** panel: Case 1 with $\lambda_\perp = 0.01$. **Top right** panel: Case 2 with $\lambda_\perp = 0.03$. **Bottom left** panel: Case 3 with $\lambda_\perp = 0.005$. **Bottom right** panel: Case 4 with $\lambda_\perp = 0.05$. All models fit the observational data and the ΛCDM model.

ent magnitude values calculating luminosity distances, we can constrain our model by comparing it with the ΛCDM.

Using Eq. (7) we know the relation between H and the θ parameter of our model. However the H parameter in Eq. (56) is a funtion of redshift z, while θ evolves through time τ, so we need to understand the relation between z and τ to perform a suitable change of variable. This relation is given by:

$$\tau = \ln \frac{1}{1+z} \;\Leftrightarrow\; z = e^{-\tau} - 1 \tag{60}$$

so,

$$\frac{\mathrm{d}z'}{\mathrm{d}\tau'} = \frac{\mathrm{d}}{\mathrm{d}\tau'}\left(e^{-\tau'} - 1\right) \implies \mathrm{d}z' = -e^{-\tau'}\mathrm{d}\tau' \tag{61}$$

Defining $\boldsymbol{\theta_0} \to 3H_0$ as:

$$\theta_0 = \sqrt{3\,(\,\rho_m(0) + \rho_\Lambda + \sigma^2(0))} \tag{62}$$

we can caltulate the luminosity distance for our model, represented as a funtion of τ, using Eqs. (7) and (56):

$$\frac{H_0\, d_L(\tau)}{c} = e^{-\tau} \int_0^\tau \frac{\theta_0}{\theta(\tau')}\, e^{-\tau'}\, \mathrm{d}\tau' \tag{63}$$

Unlike the previous simpler model, i.e. Eq. (57), this expression cannot be algebraically solved. Instead a numerical approximation must be found. In order to provide a good numerical approximation of the function, 110 points of luminosity distance were calculated.

A first comparison between the Bianchi I and ΛCDM models was made. The Bianchi I results obtained is the numerical approximation of Case 1 model for different $\lambda_\perp$ values and the new initial values and it was compared with the ΛCDM model with $\Omega_{m0} = 0.3$ and $\Omega_\Lambda = 0.7$, and represented in Figure 4. There we can see that by defining smaller values of $\lambda_\perp$ the closer the approximation between to the ΛCDM model. This is because the smaller the value of $\lambda_\perp$ the smaller the effect of anisotropic stresses in the system dynamics.

Knowing that, we now have to find values of $\lambda_\perp$ in a way that our model fits the current observable data, that is the SNIa apparent magnitude, but that some shear is still present.

Using the model of Case 1, since this is the simplest model where only one parameter must be fixed. The largest value that $\lambda_\perp$ can take in this case, without compromising the scaling regime, is given by Eq. (36) when $y_c = 1/\sqrt{3}$, so $\lambda_\perp \approx 0.05$, however this value provides

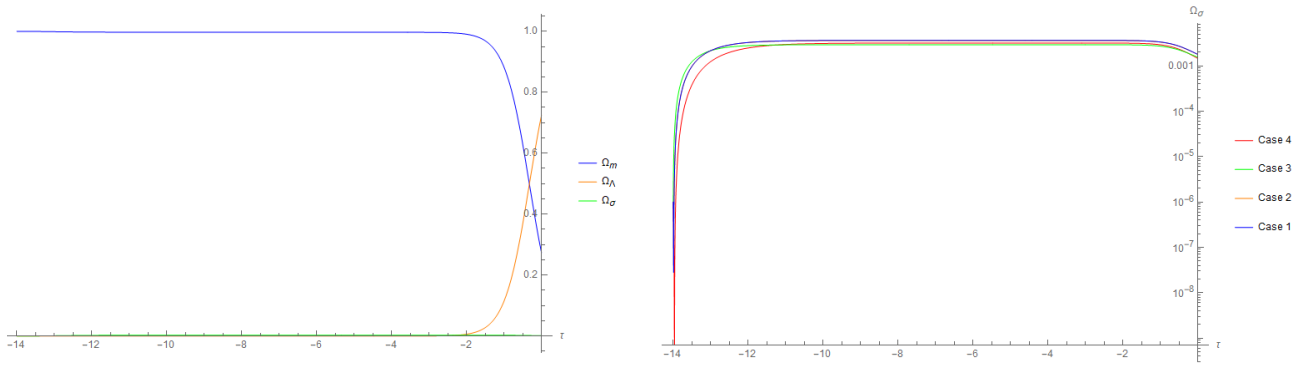

Figure 6. Bianchi I model evolution of energy-density abundances in a scaling regime compatible with present day observations. **Left** panel: Evolution of the energy-density abundance parameters - Ω_{m0}, $\Omega_{\sigma 0}$ and $\Omega_{\Lambda 0}$. Notice that the abundances remain constant during the scaling regime. **Right** panel: Comparison of the evolution of shear abundance Ω_σ between the different cases, where α was fixed at 0.1 and the $\lambda_\perp$ values at: Case 1 - 0.01, Case 2 - 0.03, Case 3 - 0.005 and Case 4 - 0.05. Dispite the differences in $\lambda_\perp$ values and anisotropic stresses form, this abundance stabilizes in similar values during the scaling regime

present energy-density abundances unlike what is observed. When $\lambda_\perp = 0.01$ the two models were very similar and the Ω abundances were similar to those at Eq. (55).

The next cases require another fixed parameter, α, so this value was fixed at $\alpha = 0.1$, in order to simplify the calculations where we find possible scaling $\lambda_\perp$ values.

For Case 2, we rearrange Eq. (41) in a way that:

$$\lambda_\perp = \frac{1}{2}\frac{y_c\left(y_c^2-1\right)}{1+y_c^2\left(\alpha-1\right)} \tag{64}$$

where $w = 0$, but we have Eq. (42), so we know that $\lambda_\perp$ can be fixed at all values until infinity and still provide a scaling solution, given enough time for the system to evolve. $\lambda_\perp = 0.03$ provided a good approximation to the current energy-density abundance data.

In Case 3 we address the problem equally using Eq. (45) and acknowledging that $|y_c| < \sqrt{1.2/3}$, and Eq. (46), we calculate that $\lambda_\perp \lessapprox 0.06$, but only values of less than 0.005 provided good approximations.

For the last case, very similar to the previous, we have that $|y_c| < \sqrt{0.8}$ given by Eq. (51), so, by Eq. (50), $\lambda_\perp \lessapprox 0.4$. When $\lambda_\perp = 0.05$ the results were close to observations

Once again these parameters are arbitrary but we intended only to find a model that roughly matches the Λ and not the best fit.

For each model, the numerical approximation of the predicted apparent magnitude was calculted using the above-mentioned values, compared with SNIa dataset and plotted as in Figure 5, where we can see that our model matches with the ΛCDM. As the represented graphs show, the evolution of energy-density parameters were very similar between the different cases and all regard the present time abundances [Eq. (55)], as we can see in Figure 6, however slight differences in the shear abundance are noticeable with a closer analysis.

Despite the differences, either in the values that $\lambda_\perp$ takes, as in the way that the anisotropic stress is defined at each case, the shear abundance stays constant, because it is a scaling solution, at roughly the same values, and a prediction of present time shear abundance $\Omega_{\sigma 0}$ can be provided in the order of 0.001.

8. CONCLUSIONS

In this work we demonstrated that axisymmetric models in Bianchi I universes with anisotropic stresses can provide stable scaling solutions that match current obervation data. As mentioned, no best fit parameter values were calculated. This is however of most importance for future work.

Continuing on that note, a more robust model can be attained by combining the different simpler cases discussed during the work in several configurations, without compromising the possibily of scaling solutions. This more complex models can be simply analysed and solved using the tools that this report provides.

Despite that, a present time shear abundance $\Omega_{\sigma 0}$ prediction was provided being its value in the order of 0.001. If the shear abundance is measured then our models can be proven and refined.

ACKNOWLEGMENTS

Thank you to the professors Nelson Nunes and José Mimoso of FCUL, that supervised this work and provided all the theoretical background and informations needed to accomplish it.

They showed how research is performed in the cosmology area of sciences and its terms. This investigation allowed me to develop problem solving skills and have a first experience in a topical research area.

REFERENCES

[1] Ellis, G. F. R. 1973. Relativistic Cosmology. Cargese Lectures in Physics 1.

[2] Damien A. Easson (2007) arXiv: astro-ph/0608034

[3] H. Hossienkhani, H. Yousefi and N. Azimi (2018) arXiv:1801.01094

[4] N. Aghanim et al. [Planck Collaboration], "Planck 2018 results. VI. Cosmological parameters," arXiv:1807.06209 [astro-ph.CO].

[5] C. W. Misner, Phys. Rev. Lett. **19**, 533-535 (1967) doi:10.1103/PhysRevLett.19.533